Nucleation barrier for phase transformations in nanosized crystals

Qingping Meng, Yonghua Rong, and T. Y. Hsu*

Department of Materials Science, Shanghai Jiao Tong University, Shanghai 200030, China

The nucleus of a new phase is considered as an inclusion embedded into a small grain of a polycrystalline matrix. The calculation of the nucleation barrier of dilatational phase transformation in nanosized crystals is carried out based on the concepts of surface stress associated with phase equilibria suggested by Cahn and Larché and the interface equilibrium given by Gurtin and Murdoch. As an example, the fcc→bcc allotropic transformation in Fe is calculated. By further addition of the shear energy using the Eshelby's shear energy equation, the nucleation barrier of martenstic transformation in nanosized crystals for Fe-30Ni alloy is calculated. The results indicate that the nucleation barrier and critical size of phase transformation in nanosized crystals are predominantly dependent on the strain energy, interphase boundary energy from phase transformation, and the grain size, however, the effect of grain size can be ignored when grain size is more than 100 nm. In the basis of these results, the different behavior of martenstic transformation between nanocrystals of Fe-Ni and NiTi alloys is reasonably explained. The factors influencing the nucleation barrier and critical sized of structural phase transformation in nanocrystals are discussed in detail.

I. INTRODUCTION

Many experiments demonstrated that the high-temperature phase (austenite) in nanosized particles often stabilize at room temperature to a great extent, as observed for free particles ranging from 10 to 200 nm in Fe-Ni alloys by Kajiwara et al.[1] and for particles with diameters of less than 10 nm in Fe-Ni films by Tadaki et al.[2,3] This phenomenon of high-temperature phase stabilization is also observed in many pure metals.[4–7] For example, the γ-Fe particle with fcc structure is found at room temperature when the size of particles is less 50 nm,[4,6] while γ-Fe in normal coarse grains will transform into α-Fe with bcc structure at 1185 K. For Co metal, Kitakami et al.[7] proved from experiment that the fcc structure remains stable at room temperature when Co particles are as small as <20 nm, while the fcc to hcp transformation takes place at 693 K in the normal coarse grains. The experiment of Zhou et al.[8] indicated that each particle (10–200 nm) in $Fe_{1-x}Ni_x$ (19 wt % <x< 32 wt %) alloys has a kind of structure bcc or fcc. The same phenomenon was found in nanosized Co particles (20–40 nm).[7] The nanosized particles in NiTi film in contrast to that in Fe-Ni alloy could not suppress the martensitic transformation.[9,10] Obviously, there may be a noticeable difference about the effect of particle (grain) size on martensitic transformation (or the stability of austenite) between them.

The nanocrystalline materials are structurally characterized by ultrafine grains and a large volume fraction of interface, such as grain boundary, phase, and domain interfaces, etc. These interfaces should affect the behavior of phase transformation in nanocrystals. Cahn et al.[11,12] have proposed that the action of the surface stress in solid relates to the work of deforming the surface elastically and affects strain energy and interfacial energy from phase transformation. But they only considered the equilibria of an inclusion (such as a new phase nucleus) embedded in an infinite solid matrix. In the case of an inclusion embedded in a nanosized grain of polycrystals, the effect of grain boundary stress should be noted.

The present article attempts to calculate the nucleation barrier of phase transformations in nanosized crystals based on the concepts of surface stress associated with phase equilibria suggested by Cahn and Larché[11,12] and the interface equilibrium given by Gurtin and Murdoch[13] for dilatational transformation as well as addition of shear energy by using Eshelby's equation[14] for martensitic transformation. As examples, the nucleation barriers of allotropic transformation of Fe and martensitic transformation of Fe-30Ni in nanosized crystals are calculated, and factors influencing the nucleation barrier of phase transformations in nanocrystals will be discussed in detail, from which the difference behavior of phase transformations between nanosized grains and normal coarse grains and that of martensitic transformation between Fe-Ni and NiTi alloys will be reasonably explained.

In nanosized crystals, nucleation for diffusional phase transformation on grain boundaries may also be preferential to that inside a grain. In the present work, we will only consider the homogeneous nucleation within a grain, but not discuss the nucleation on grain boundaries. For the martensitic transformation, the nucleation on grain boundaries can be ignored due to the displacive character of martensitic transformation.

II. THE NUCLEATION BARRIER FOR DILATATIONAL PHASE TRANSFORMATION IN NANOSIZED CRYSTAL

The nucleus of a new phase (α) in nanosized crystals can be considered as an inclusion embedded in a small spherical grain (γ) of a polycrystal matrix (M) as shown in Fig. 1. Obviously, an interphase boundary between α and γ and a grain boundary between γ and M exists.

The change in free energy for phase transformation can be written as

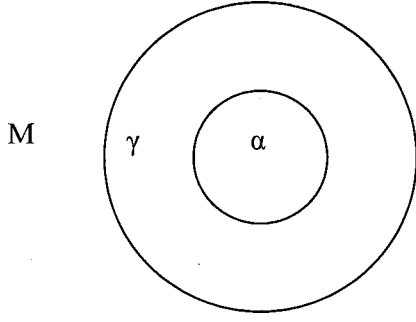$$\Delta G = V\Delta G_{\gamma-\alpha} + E_{sto}, \tag{1}$$

FIG. 1. Schematic illustration of a new phase (α) embedded in a small spherical grain (γ) of polycrystal matrix (M).

where $\Delta G_{\gamma-\alpha}$ is the change in free energy per unit volume accompanying $\gamma \rightarrow \alpha$, V is the volume of the new phase, and E_{sto} is the store energy arising from strain energy and interfacial energy produced by phase transformation, generally including strain energy in individual α, γ, M and interface energies $E^{\alpha-\gamma}$ and $E^{\gamma-M}$ between $\alpha-\gamma$ and $\gamma-M$, respectively. The calculation of strain energy and interfacial energy in the nanosized crystals is different from the normal bulk materials because the influence of interface stress on grain boundary cannot be ignored.

Accompanying reconstructive transformation, the change of volume in new phase relative to a parent phase is usually produced, while in displacive transformation the shear strain must also be added. In this section, only the dilation case will be referred to. In Fig. 1 we choose the stress-free states of α and γ as their respective reference state at zero pressure, and assume that the infinite matrix phase and the new phase are isotropic. In this state α has a radius R_0^α and γ a hole of radius R_0, with

$$R_0^\alpha = (1+\varepsilon)R_0, \tag{2}$$

where ε represents the dilatational strain of α relative to γ.

According to the method of Eshelby[14] and the symmetry of sphere, we know that the stress field is only a function of radius r. Therefore, the equations of displacement equilibrium[15] is

$$\frac{\partial^2 \omega}{\partial r^2} + \frac{2}{r}\frac{\partial \omega}{\partial r} - \frac{2\omega}{r^2} = 0. \tag{3}$$

Its general solution is

$$\omega = Ar + B/r^2. \tag{4}$$

The values of A and B can be determined from boundary conditions. In the new phase (α), $B=0$, because displacement ω should be finite when $r\rightarrow 0$, and for the same reason, $A=0$ in the matrix (M), while in a small grain (γ), both A and B are not equal to zero. The ω in α, γ, and M are, respectively,

$$\omega^{\alpha'} = C_1 \varepsilon r \quad (r<R_0), \tag{5}$$

$$\omega^\gamma = C_2 r + C_3/r^2 \quad (R_0<r<R_1), \tag{6}$$

and

$$\omega^M = C_4/r^2 \quad (r>R_1), \tag{7}$$

where the superscripts α, γ, and M stand for the new phase, small grain, and matrix, respectively. R_1 is the radius of the small grain. From Eq. (5), the contracting displacement of the free expansion α phase resulting from the constrain of the γ phase is $\omega^\alpha = \varepsilon(C_1-1)r$, and for this state the stress (pressure)[12,16] in α is

$$P = 3K^\alpha(C_1-1)\varepsilon, \tag{8}$$

the stress in γ is determined as follows:

$$\sigma_{rr}^\gamma = \frac{3\lambda^\gamma C_2 r^3 + 2\mu^\gamma C_2 r^3 - 4\mu^\gamma C_3}{r^3}, \tag{9}$$

$$\sigma_{\theta\theta}^\gamma = \sigma_{\varphi\varphi}^\gamma = \frac{3\lambda^\gamma C_2 r^3 + 2\mu^\gamma C_2 r^3 + 2\mu^\gamma C_3}{r^3}, \tag{10}$$

and the stress in M is

$$\sigma_{rr}^M = -4\frac{\mu^\gamma C_4}{r^3}, \tag{11}$$

$$\sigma_{\theta\theta}^M = \sigma_{\varphi\varphi}^M = 2\frac{\mu^\gamma C_4}{r^3}, \tag{12}$$

where K^α, λ^γ, and μ^γ are the bulk modulus of α and Lamé constants of γ, respectively. C_1, C_2, C_3, and C_4 are obtained by the following boundary conditions.

Gurtin and Murdoch[13] deduced the mechanical balance of forces at the interface

$$\sigma^\alpha \cdot \mathbf{n}^\alpha + \sigma^\beta \cdot \mathbf{n}^\beta - \text{div } \mathbf{f} = \mathbf{0}, \tag{13}$$

where superscripts α and β show, respectively, two different phases (or grains) in the sides of an interface, σ^α and σ^β are the stress tensors of these two phases (or grains), respectively, $\mathbf{n}^\alpha$ and $\mathbf{n}^\beta$ are the exterior normal to α and β ($n^\alpha = -n^\beta$), respectively, $\mathbf{f}$ is the surface stress tensor, and div is the surface divergence. In the spheric symmetry case, the components of $\mathbf{f}$ are $f_{\theta\theta}=f_{rr}=f$ (Ref. 12) and

$$\text{div } \mathbf{f} = -2f\mathbf{n}^\beta/R, \tag{14}$$

where R is the radius of interface. The equations of mechanical balance of $\alpha-\gamma$ and $\gamma-M$ interfaces are obtained from Eq. (13),

$$\frac{3\lambda^\gamma C_2 R_0^3 + 2\mu^\gamma C_2 R_0^3 - 4\mu^\gamma C_3}{R_0^3} = 3K^\alpha \varepsilon(C_1-1) + 2f_1/R_0, \tag{15}$$

$$-4\frac{\mu^\gamma C_4}{R_1^3} = \frac{3\lambda^\gamma C_1 R_0^3 + 2\mu^\gamma C_2 R_1^3 - 4\mu^\gamma C_3}{R_1^3} + 2f_2/R_1, \tag{16}$$

where f_1 and f_2 are, respectively, the interface stresses of $\alpha-\gamma$ and $\gamma-M$. In the isotropic case, their values are equal to their interfacial energy.[17,18] The equations of the normal

displacement continuum of $\alpha - \gamma$ and $\gamma - M$ interfaces can be obtained from equations (5)–(7):

$$C_2 R_0 + \frac{C_3}{R_0^2} = C_1 \varepsilon R_0, \qquad (17)$$

$$C_2 R_1 + \frac{C_3}{R_1^2} = \frac{C_4}{R_1^2}. \qquad (18)$$

The strain energy densities of α, γ, and M can be calculated from the basic formula of elastic mechanics, respectively,

$$e^\alpha = \frac{3}{2} K^\alpha (C_1 - 1)^2 \varepsilon^2, \qquad (23)$$

$$e^\gamma = \frac{3}{2} C_2^2 (3\lambda^\gamma + 2\mu^\gamma) + 6\mu^\gamma C_3^2 / r^6, \qquad (24)$$

$$e^M = \frac{6\mu^\gamma C_4^2}{r^6}. \qquad (25)$$

The strain energies stored in an individual solid can be calculated by a volume integration of their strain energy density

$$E^\alpha = 2\pi K^\alpha (C_1 - 1)^2 \varepsilon^2 R_0^3, \qquad (26)$$

$$E^\gamma = -\frac{2\pi [R_1^3 R_0^3 C_2^2 (3\lambda^\gamma + 2\mu^\gamma) + 4\mu^\gamma C_3^2](R_0^3 - R_1^3)}{R_0^3 R_1^3}, \qquad (27)$$

$$E^M = \frac{8\pi\mu^\gamma C_4^2}{R_1^3}. \qquad (28)$$

The total strain energy from the dilatational strain of the new phase is

$$E_s = E^\alpha + E^\gamma + E^M. \qquad (29)$$

Cahn and Larché[7] gave the calculated formula of interfacial energy (interfaces are assumed to be coherent):

$$\gamma = \gamma_0 + f_{ij} \varepsilon_{ij}, \qquad (30)$$

where γ_0 is the interfacial energy when the strain is zero. $f_{ij} = f\delta_{ij}$ in the isotropic case, then the interfacial energy of $\alpha - \gamma$ or $\gamma - M$ becomes

Solving equations (15)–(18), C_1, C_2, C_3, and C_4 are, respectively,

$$C_1 = -\frac{2 f_1 R_1 - 3R_0 R_1 \varepsilon K^\alpha + 2R_0 f_2}{R_0 R_1 \varepsilon (4\mu^\gamma + 3K^\sigma)}, \qquad (19)$$

$$C_2 = -\frac{2 f_2}{3R_1 (\lambda^\gamma + 2\mu^\gamma)}, \qquad (20)$$

$$C_3 = -\frac{1}{3} \frac{R_0^2 [6R_1 f_1 (\lambda^\gamma + 2\mu^\gamma) - 9R_0 R_1 \varepsilon K^\alpha (\lambda^\gamma + 2\mu^\gamma) + 2R_0 f_2 (2\mu^\gamma + 3\lambda^\gamma) - 6R_0 f_2 K^\alpha]}{R_1 (\lambda^\gamma + 2\mu^\gamma)(4\mu^\gamma + 3K^\sigma)}, \qquad (21)$$

$$C_4 = -\frac{1}{3} \frac{2 f_2 R_1^3 (3K^\alpha + 4\mu^\gamma) + 2R_0^3 f_2 (2\mu^\gamma + 3\lambda^\gamma - 3K^\alpha) + 3R_0^2 R_1 (2 f_1 - 3R_0 \varepsilon K^\alpha)(\lambda^\gamma + 2\mu^\gamma)}{R_1 (\lambda^\gamma + 2\mu^\gamma)(3K^\alpha + 4\mu^\gamma)}. \qquad (22)$$

$$E^{\alpha-\gamma} = S^{\alpha-\gamma}(\gamma_0^{\alpha-\gamma} + 2 f_1 C_1 \varepsilon) = 4\pi R_0^2 (\gamma_0^{\alpha-\gamma} + 2 f_1 C_1 \varepsilon), \qquad (31)$$

$$E^{\gamma-M} = S^{\gamma-M} \left(2C_2 f_2 + \frac{2C_3 f_2}{R_1^3} \right) = 8\pi R_1^2 \left(C_2 f_2 + \frac{C_3 f_2}{R_1^3} \right), \qquad (32)$$

where $S^{\alpha-\gamma}$ and $S^{\gamma-M}$ are the interface areas of $\alpha - \gamma$ and $\gamma - M$, respectively.

Accordingly, the store energy produced by the formation of a new phase can be written as

$$E_{\text{sto}} = E_s + E^{\alpha-\gamma} + E^{\gamma-M}. \qquad (33)$$

Prior to phase transformation, the stress of grain boundary between $\gamma - M$ also brings about the strain energy in the small grain and polycrystalline matrix, and the change in grain boundary energy due to elastic strain in the solids resulting from f_2. By using the same method mentioned above, the strain energy E_{pri}^γ in γ, E_{pri}^M in M, and the change of grain boundary energy $E_{\text{pri}}^{\gamma-M}$ from the stress of grain boundary are deduced as

$$E_{\text{pri}}^\gamma = \frac{8\pi}{9} \frac{R_1 f_2^2 (3\lambda^\gamma + 2\mu^\gamma)}{(\lambda^\gamma + 2\mu^\gamma)^2}, \qquad (34)$$

$$E_{\text{pri}}^M = \frac{32\pi}{9} \frac{R_1 f_2^2 \mu^\gamma}{(\lambda^\gamma + 2\mu^\gamma)^2}, \qquad (35)$$

$$E_{\text{pri}}^{\gamma-M} = -\frac{16\pi}{3} \frac{R_1 f_2^2}{\lambda^\gamma + 2\mu^\gamma}. \qquad (36)$$

These energy items should be added to Eq. (1) for dealing with phase transformation in nanosized grains. Therefore, the change in free energy accompanying the $\gamma \rightarrow \alpha$ transformation in small grain can be written as

$$\Delta G = V\Delta G_{\gamma-\alpha} + E_{\text{sto}} - (E_{\text{pri}}^\gamma + E_{\text{pri}}^M + E_{\text{pri}}^{\gamma-M}) \qquad (37)$$

TABLE I. The required parameters of Fe and Fe-30Ni.

Parameters	Notation	Unit	Fe	Fe-30Ni
Lattice parameter fcc structure	a_γ	Å	3.56[a]	3.5854[e]
Lattice parameter bcc structure	a_α	Å	2.86[a]	2.8635[e]
Elastic constant of fcc structure	C_{11}	10^{10} Pa	14.1[b]	14.75[f]
	C_{12}	10^{10} Pa	10.0[b]	8.92[f]
	C_{44}	10^{10} Pa	10.8[b]	11.31[f]
Lamé constant of fcc structure	μ	10^{10} Pa	4.00[i]	5.26[i]
	λ	10^{10} Pa	8.70[i]	8.04[i]
Poisson's ratio of fcc structure	ν		0.34[i]	0.30[i]
Young's modulus of bcc structure	E	10^{10} Pa	21.14[c]	15.3[g]
Shear modulus of bcc structure	μ	10^{10} Pa	8.18[c]	5.50[g]
Bulk modulus of bcc structure	K	10^{10} Pa	16.98[c]	19.7[i]
Free energy difference (at 0 K)	$\Delta G_{\gamma-\alpha}$	10^8 J/m^3	4.08[d]	2.88[h]
Dilation of fcc→bcc transformation	ε		0.037	0.018
Shear strain of martensitic transformation	ε_{sh}			0.22

[a]Ref. 23.
[b]Ref. 24.
[c]Ref. 25.
[d]Ref. 26.
[e]Ref. 27.
[f]Ref. 28.
[g]Ref. 29.
[h]Ref. 30.
[i]Calculated values from other elastic constants.

III. THE CALCULATION OF NUCLEATION BARRIER FOR DILATATIONAL PHASE TRANSFORMATION IN NANOSIZED CRYSTAL

In reconstructive transformations, the appearance of a new phase will produce the change of volume and will build a new interface. For example, the dilation of volume in fcc →bcc allotropic change of Fe is 3.7%, which is calculated by the lattice parameters of α-Fe and γ-Fe. As an application of Sec. II, the nucleation barrier of fcc→bcc transformation in Fe will be calculated. The required parameters for calculation of the nucleation barrier in Fe are listed in Table I.

The grain boundary energy in nanosized crystals is usually larger than that in bulk materials,[19–21] but the actual value has not been reported. In the present article the energy of the high-angle grain boundary in coarse grains is approximately taken as that of grain boundary in nanocrystals. Wolf[22] calculated the energy of high-angle grain boundary of α-Fe and obtained the energy of (100) boundary is about 1.6 J/m^2. Since the interface is assumed to be isotropic, the numerical value of specific interface energy (per unit area) is equal to that of interface stress.[17,18] The interphase boundary energy is usually lower than grain boundary energy. Although the different approximate values of interfacial energy will be employed in our calculations, it does not affect the correctness of the calculated results except for its precision.

Figure 2, the result of calculation by Eq. (37), shows the free energy change of fcc→bcc (ΔG) with the radius of bcc embryos (R_0) in Fe. It can be found from Fig. 2 that with a decrease of the grain radius, the nucleation barrier for fcc →bcc ΔG^c and critical radius of nucleation R_0^c (the R_0 corresponding to peak value in Fig. 2) will increase. It indicates that the decrease of the grain size is favorable for the stability of γ-Fe with fcc structure. It is worthy noting that critical

radius of nucleation R_0^c is larger than grain radius R_1 when R_1 is enough small, the result can be deduced that in so small nano-sized crystal, once phase transformation occurs the whole grain of γ-Fe will transform into that of α-Fe, that is, in this case the bcc and fcc phase cannot coexist in the same grain.
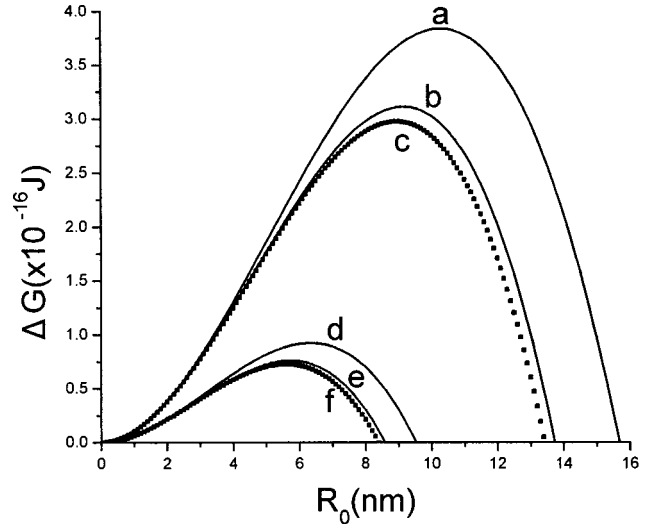

FIG. 2. Relationship between the free energy of fcc→bcc transformation and the bcc phase nuclear size in iron with different grain radius R_1, interphase boundary energy f_1, and a given grain boundary energy $f_2 = 1.6$ J/m^2. The squares represent Cahn and Larché work. (a) $f_1 = \gamma_0^{\alpha-\gamma} = 0.8$ J/m^2, $R_1 = 10$ nm; (b) $f_1 = \gamma_0^{\alpha-\gamma} = 0.8$ J/m^2, $R_1 = 50$ nm; (c) $f_1 = \gamma_0^{\alpha-\gamma} = 0.8$ J/m^2; (d) $f_1 = \gamma_0^{\alpha-\gamma} = 0.5$ J/m^2, $R_1 = 10$ nm; (e) $f_1 = \gamma_0^{\alpha-\gamma} = 0.5$ J/m^2, $R_1 = 50$ nm; (f) $f_1 = \gamma_0^{\alpha-\gamma} = 0.5$ J/m^2.

IV. THE NUCLEATION BARRIER OF MARTENSITIC TRANSFORMATION IN NANOSIZED Fe-Ni ALLOYS

In the above calculation only the strain energy and interfacial energy of the spherical symmetry are considered. Martensitic transformation usually produces the dilation of volume as well as shear strain. Therefore, the shear strain energy E_{sh} must be added in the store energy E_{sto} for calculation of nucleation barrier. The shear strain energy of martensitic transformation is dependent on the shape of the martensitic nuclei. However, the shape of martensitic nuclei strongly depends on the composition of an alloy. For example, in steels with $<0.2\%$ carbon and $<29\%$ nickel content, the shape of martensite is the lath, while in high carbon and high nickel steels it is lenticular.[31] For the martensitic transformation, the spherical symmetry will disappear, and the calculation will become very complicated if the influence of interface stress on shear strain is considered. For the sake, as a rough approximation, which can give a tendency of nucleation barrier of martensitic transformation with strain energy, the formula of shear strain energy given by Chistian[32] based on Eshelby inclusion theory[14] is directly expressed as

$$E_{sh} = \frac{\pi(2-\nu)G}{8(1-\nu)} \frac{c}{\alpha} \varepsilon_{sh}^2, \qquad (38)$$

where ν is Poisson's ratio, ε_{sh} is the shear strain of martensitic transformation, c/a is the semithickness/radius ratio of the oblate spheroidal nuclei of martensite. The shear energy is linearly proportional to c/a, thus the maximal shear energy corresponds to the sphere shape, the minimal does the lath. The small value of c/a significantly decreases the shear energy, but somewhat increases the interfacial energy.

The shape of martensite in a bulk Fe-30Ni alloy was observed as to be lenticular, and its c/a is about $\frac{1}{50}$.[33] While in Fe-Ni alloys with a low Ni content (<29 at. %) the lath martensite appears, and its c/a is much smaller than that of lenticular martensite.

The parameters of Fe-30Ni alloy for calculating the nucleation barrier of martensitic transformation also are listed in Table I, in which the dilation of volume and shear strain value of martensitic transformation is calculated by the lattice parameter and WLR theory,[34] respectively.

The curve a in Fig. 3 shows that the free energy change (ΔG) accompanying the martensitic transformation relates with the martensitic embryo radius R_0 when the shear strain energy is added into the store energy in Eq. (33). In order to emphasize the effect of shear strain, the curve b that excluded the shear strain is also drawn in Fig. 3. Figure 3 indicates that the nucleation barrier ΔG^c and critical radius of nucleation R_0^c rapidly increase with the increase of shear strain energy.

V. DISCUSSION

A. Effect of the grain size on nucleation barrier and critical radius of nucleation

Figure 2 shows that the change in Gibbs free energy (ΔG) depends on the size of nuclei (R_0) in Fe with grains of
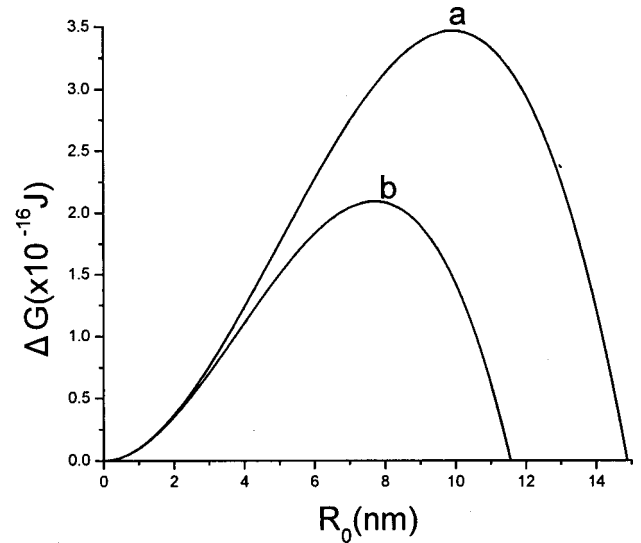

FIG. 3. Relationship between the free energy of martensitic transformation and the martensitic nuclear size in Fe-30Ni alloy with a given grain radius $R_1 = 50$ nm, interphase boundary energy $f_1 = \gamma_0^{\alpha-\gamma} = 0.8$ J/m^2 and grain boundary energy $f_2 = 1.6$ J/m^2. The shear strain energy with $c/a = \frac{1}{50}$ is considered in curve a, not in curve b.

50 and 10 nm radius (R_1) and for a given value of the interphase boundary energy. The change in Gibbs free energy of dilatational phase transformation in infinite grain from Cahn and Larché[12] are also shown in Fig. 2 for comparison. It can be found from Fig. 2 that our calculated results are almost the same as Cahn and Larché's work when the grain radius exceeds 50 nm. ΔG^c increases evidently with the decrease of the grain radius from 50 to 10 nm, but R_0^c increases slightly. The effect of grain size on free energy is not so evident when a grain radius is more than 50 nm in Fe.

B. Effect of interphase boundary energy on nucleation barrier and critical radius of nucleation

There is an interphase boundary between a new phase and a parent phase. The magnitude of the interphase boundary energy depends on several factors, such as the structure of interface, coherence degree of interface and the shape of a new phase etc. It can be found from Fig. 2 that the $\Delta G - R_0$ curve is intensively affected by the interphase boundary energy. ΔG^c and R_0^c increase rapidly with the slight increase of interphase boundary energy from 0.5 to 0.8 J/m^2 for a given grain size (10 or 50 nm). It indicates that the interphase boundary energy plays an important part in phase transformation of nanosized grains.

C. Effect of the shear energy on nucleation barrier and critical radius of nucleation

As mentioned above, the shear energy strongly depends on the shape of martensitic nucleus. Figure 4 shows the relationship among the nucleation barrier ΔG^c, critical radius of nucleation R_0^c, and the c/a ratio of ellipsoid nucleus in the Fe-30Ni alloy. In Fig. 4, ΔG^c and R_0^c greatly increase
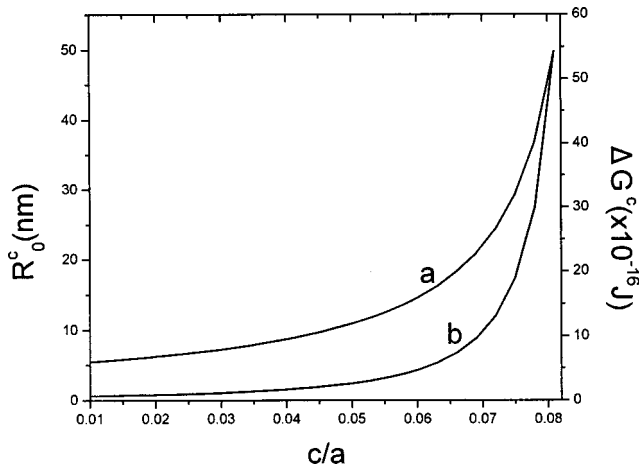
FIG. 4. Dependence of the critical nucleation size R_0^c and nucleation barrier ΔG^c with martensitic transformation on an increase of strain energy in Fe-30Ni alloy for $R_1 = 50$ nm, interphase boundary energy $f_1 = \gamma_0^{\alpha - \gamma} = 0.5$ J/m^2 and grain boundary energy $f_2 = 1.6$ J/m^2. (a) $c/a - R_0^c$; (b) $c/a - \Delta G^c$.

with the slight increase of c/a ratio due to the increase of the shear strain energy. As a consequence, the increase of the c/a ratio of ellipsoid nucleus will strongly suppress the martensitic transformation.

D. The comparison of martensitic transformation of nanosized crystal in Fe-Ni alloy within NiTi alloy

From the above discussion both the nucleation barrier ΔG^c and critical radius of nucleation R_0^c depend on the interphase boundary energy and strain energy produced from the phase transformation as well as the parent grain size. ΔG^c and R_0^c increase slightly with the decrease of grain size, but the ΔG^c and R_0^c obviously increase with the increase of the interphase boundary energy or the strain energy as shown in Figs. 2–4. The strain energy arising from phase transformation relates to the difference of physical and mechanical parameters between new and parent phases as well as magnitude of strain. Since the dilatational stain in martensitic transformation of NiTi shape memory alloy is very small $(<1\%)$,[35] and the c/a of martensite is also very small, meanwhile, in NiTi alloy the total shear stain tends to be zero due to the self-accommodation of martensite variants, the nucleation barrier of martensitc transformation is too small to suppress the occurrence of martensitic transformation in nanosized NiTi, which has been verified by the experiments.[9,10] In

contrast, in Fe-Ni alloys such as Fe-30Ni, the volume dilatation (near 2%) of martensite is much larger than that of NiTi alloy, accordingly, it is conceivable that the martensitic transformation in nanocrystalline Fe-30Ni becomes difficult, and the same behavior occurs in martensitic transformation of nano-ZrO$_2$ ceramic with about 5% volume dilatation.[36]

VI. CONCLUSIONS

The nucleus of a new phase is considered as an inclusion embedded into a small grain of a polycrystalline matrix. The calculation of nucleation barrier for dilatational phase transformation, such as allotropic transformation of Fe, and the critical radius of nucleation in nanosized crystals was carried out based on the concepts of surface stress associated with phase equilibria suggested by Cahn and Larché and the interface equilibrium given by Gurtin and Murdoch. By further addition of the shear energy using the Eshelby's shear energy equation the nucleation barrier of martenstic transformation in nanosized crystals for Fe-30Ni as an example was calculated. The conclusions are summarized as follows.

(1) The nucleation barrier and the critical nucleation size of new phase depend on the parent grain size for a given grain boundary energy, as well as a given interphase boundary energy and strain energy arising from phase transformation. The effect of grain size on the nucleation barrier and critical nucleation size cannot been ignored when the grain diameter is less than 100 nm. The effect of interphase boundary energy and strain energy on the nucleation barrier as well as the critical size of nucleation is evident, so the low phase interface energy and strain energy are favorable for phase transformation in nanocrystalline materials, from which it can be explained the fact that the occurrence of martensitic transformation in nanosized NiTi alloys is easier than that in Fe-Ni alloys.

(2) In nanocrystalline materials, the critical nucleation size of the new phase will be larger than the grain size of parent phase when the grain size is enough small. In this case, once phase transformation takes place, the whole grain will transform from parent phase into new phase, indicating the two phases can not coexist in such a small grain.

ACKNOWLEDGMENTS

*Author to whom correspondence should be addressed. Electronic address: zyxu@mail1.sjtu.edu.cn

[1] S. Kajiwara, S. Ohno, and K. Honma, Philos. Mag. A **63**, 625 (1991).

[2] T. Tadaki, Y. Murai, A. Koreeda, Y. Nakata, and Y. Hirotsu, Mater. Sci. Eng., A **217-218**, 235 (1996).

[3] K. Asaka, Y. Hirotsu, and T. Tadaki, Mater. Sci. Eng., A **273-275**, 262 (1999).

[4] Y. Fukano, Jpn. J. Appl. Phys. **13**, 1001 (1974).

[5] C. G. Granqvist and R. A. Buhrman, J. Appl. Phys. **47**, 2200 (1976).

[6] K. Haneda, Z. X. Zhou, and A. H. Morrish, Phys. Rev. B **46**, 13 832 (1992).

[7] O. Kitakami, H. Sato, and Y. Shimada, Phys. Rev. B **56**, 13 849 (1997).

[8] Y. H. Zhou, M. Harmelin, and J. Bigot, Mater. Sci. Eng., A **124**, 241 (1990).

[9] Y. Qin, L. Chen, Y. Zhu, and L. Zhang, J. Mater. Sci. Lett. **15**,

1155 (1996).

[10] T. Kikuchi, K. Ogawa, S. Kajiwara, T. Matsunaga, S. Miyazaki, and Y. Tomota, Philos. Mag. A **78**, 467 (1998).

[11] J. W. Cahn, Acta Metall. **28**, 1333 (1980).

[12] J. W. Cahn and F. Larché, Acta Metall. **30**, 51 (1982).

[13] M. Gurtin and A. I. Murdoch, Arch. Ration. Mech. Anal. **57**, 291 (1975).

[14] J. D. Eshelby, Proc. R. Soc. London, Ser. A **241**, 376 (1957).

[15] J. W. Christian, *The Theory of Transformations in Metals and Alloys* (Pergamon, Oxford, 1975), p. 202.

[16] N. Mott and F. R. N. Nabarro, Proc. Phys. Soc. London **51**, 86 (1940).

[17] D. W. Hoffman and J. W. Cahn, Surf. Sci. **31**, 368 (1972).

[18] J. W. Cahn and D. W. Hoffman, Acta Metall. **22**, 1205 (1974).

[19] H. J. Fecht, Phys. Rev. Lett. **65**, 610 (1990).

[20] M. Wagner, Phys. Rev. B **45**, 635 (1992).

[21] K. Lu, Phys. Rev. B **51**, 18 (1995).

[22] D. Wolf, Philos. Mag. B **59**, 667 (1989).

[23] *Smithells Metals Reference Book*, edited by E. A. Brandes (Butterworths, London, 1983), p. 6-4.

[24] M. Grujicic and X. W. Zhou, CALPHAD: Comput. Coupling Phase Diagrams Thermochem. **17**, 383 (1993).

[25] *Smithells Metals Reference Book*, edited by E. A. Brandes (Butterworths, London, 1983), p. 15-2.

[26] M. I. Baskes, Phys. Rev. B **46**, 2727 (1992).

[27] A. J. Goldman and C. N. J. Wagner, Acta Metall. **11**, 405 (1963).

[28] G. A. Alers, J. R. Neighbour, and H. Sato, J. Phys. Chem. Solids **13**, 40 (1960).

[29] A. J. Goldman and W. D. Robertson, Acta Metall. **12**, 1265 (1964).

[30] L. Kaufman and M. Cohen, Trans. AIME **206**, 1393 (1956).

[31] T. Y. Hsu (Xu Zuyao), *Martensitic Transformation and Martensite*, 2nd ed. (Science Press, 1999) (in Chinese).

[32] J. W. Christian, Acta Metall. **6**, 377 (1958).

[33] A. J. Goldman and W. D. Robertson, Acta Metall. **13**, 391 (1965).

[34] M. S. Wechsler, D. S. Lieberman, and T. A. Read, Trans. AIME **197**, 1503 (1953).

[35] F. Falk, Z. Phys. B: Condens. Matter **51**, 177 (1983).

[36] J. D. McCullough and K. N. Trueblood, Acta Crystallogr. **18**, 983 (1965).